

PHYSICAL MODELLING AND PROFILE OPTIMIZATION OF SINGLE- AND DOUBLE-IMPLANT GAAS MESFETS *

Giovanni Ghione*, Carlo U. Naldi^o

* Dipartimento di Elettronica, Politecnico di Milano

^o Dipartimento di Elettronica, Politecnico di Torino

A. Cetronio,
SELENIA S.p.A, Roma

Abstract

The paper addresses a few issues concerning the two-dimensional physical simulation of ion-implanted MESFET devices. The simulation of implanted profiles is briefly discussed, and simple models are proposed for the transport properties of carriers in the presence of residual acceptor-like impurities. Finally, the problem of optimizing the performances of double-implant MESFETs is treated. Comparisons with experimental results are made throughout the paper.

1 Introduction

Ion-implanted GaAs MESFETs are under many respects more complex to simulate than abrupt-doping (epitaxial) devices. First, an accurate simulation of the activated doping profile resulting from multiple ion implants followed by annealing cannot be performed any longer on the basis of a restricted set of parameters (basically, the dopant concentration in the epitaxial layer, the residual impurity background of the substrate and the depth of the transition between them) but requires a detailed knowledge of the technological process and the development of a simple *process simulator*.

Second, heavily compensated substrates or substrates with high level of residual impurities play a greater role on the device performances near pinchoff than in epitaxial devices. This requires that the influence of impurities be accounted for when evaluating the transport properties of carriers in the active layer-substrate transition [7,10,15].

Finally, *profile optimization* does not abide by simple rules, as for epitaxial devices, since the possibility of performing *variable energy* and *multiple* implants

* Work partly supported by Selenia S.p.A

allows the designer a higher degree of freedom. On the other hand, the possibility of tuning the profile so as to achieve a prescribed goal (e.g. optimizing the transconductance, or the device bandwidth) opens up interesting possibilities to *physical device simulation* [2,7,9,14].

In the present paper, several issues concerning the two-dimensional physical simulation of ion-implanted MESFETs are addressed. First, the evaluation of the input doping profile is discussed; then, simple models for the carrier transport properties, accounting for the presence of a residual acceptor background, are presented. Finally, it is shown how a two-dimensional simulator (MESS, see [6]) can be used as a tool for the optimization of double-implant devices. Since 2D simulation is comparatively CPU intensive, its use within an optimization process is mainly meant to allow the designer a better insight on the device behaviour and to improve the result already obtained with a coarse preliminary optimization based on analytical or quasi-physical models. The conclusions reached through numerical simulation are supported by measurements on devices manufactured by SELENIA.

An extensive presentation on the MESS simulator can be found in [6]. Here we only recall that MESS implements the steady-state and small-signal simulation of planar and recessed-gate MESFETs¹. The physical model is the *diffusion model*, and the discretization and solution are based on the well-known Scharfetter-Gummel discretization on a triangular grid, coupled with Newton-Richardson techniques for the computation of the working point. Direct linearization is used to deal with the small-signal simulation. The simulator accepts arbitrary doping and initial mobility profiles.

2 Profile simulation

As well known, the doping profile of an ion implanted device is determined not only by the characteristics of the implant itself (i.e.: implanted material, dose, and implant energy) but also by the *annealing* time and temperature. Although the experimental approach is of course the simplest and more accurate solution to profile modelling, reliable measurements on implanted profiles (e.g. SIMS measurements) are not always available. Therefore, the need arises of generating the input doping profile through a simple *process simulator*.

In the present research, the implanted profile (before annealing) has been simulated by means of Pearson IV distributions [12,13]². In fact, Gaussian distributions are often unsatisfactory, since they not reproduce the asymmetry and the non-exponential tails which are found in measured profiles. Unfortunately, the Pearson IV distribution requires *four* input parameters: the *projected range* R_p , the *standard deviation* σ_p , the *skewness* γ and *kurtosis* β . The skewness is a measure of the asymmetry of the distribution with respect to its maximum: for $\gamma > 0$, the a steeper profile towards the surface is obtained, whereas for $\gamma < 0$ the profile is steeper toward the bulk [12]. The *kurtosis* coefficient has little influence

¹An extension to more general geometries (e.g. double-recess devices) is actually in progress.

²The same kind of distribution was used in the GaAs oriented version of the SUPREM simulator [1].

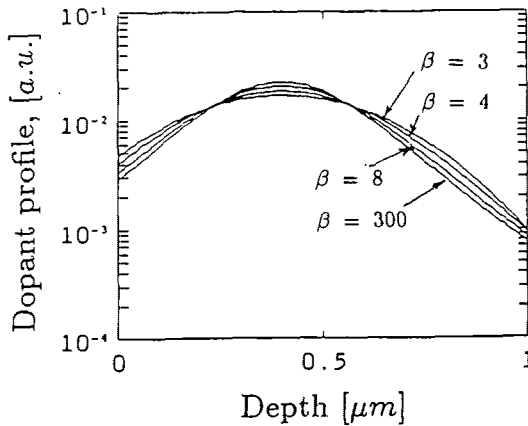


Figure 1: Effect of kurtosis on almost symmetric Pearson IV distribution

on the shape of the distribution. Large values of β lead to a more peaked distributions, as shown in Fig.1 for a distribution with zero skewness. Notice that for $\beta = 3$ a Gaussian profile is obtained, and that varying the kurtosis has no influence on the symmetry of the distribution³. The Gaussian profile is therefore always *blunter* than the Pearson IV profile.

While the dependence of R_p and σ_p on implant energy is available for many practically important dopants [16] under the form of tabulated values, which can be easily curve fitted (cfr. Fig.2), very little information can be found on the parameters γ and β for GaAs substrates. Therefore, such parameters had to be newly estimated by fitting experimental results, taken both from SELENIA measurements and from published data [1]. Since all devices of interest were obtained through Si implants, we restrict ourselves to discussing the behaviour of this dopant.

As a general remark, good agreement was found for the projected range and standard deviation between measurements and published data. However, the curves found in [1] show slightly higher values than expected; in particular, the standard deviation observed is closer to the value expected for the *lateral straggle* [16]⁴. Concerning *skewness*, good fits are obtained with rather small values (e.g. $\gamma = 0.1 - 0.3$) which *increase* with implant energy (See Fig.3). The *kurtosis* resulting from fitting is (as expected) the noisiest parameter; at any rate, comparatively high values (e.g. $\beta = 10 - 15$) lead to the optimum fit. Some care should be used when assigning values to β , since this parameter must satisfy some limitations in order to be compatible with a Pearson IV distribution (cfr. e.g. [13], eq.(3.1-42)). In particular, one must always have $\beta > 3$, and the minimum value is reached when the skewness is zero (Gaussian distribution). The empirical formula $\beta \approx 2.8 + 2.4\gamma^2$ originally proposed in [11] and also suggested

³The coefficient β is connected to the *fourth* moment of the distribution with respect to its maximum.

⁴The profiles shown in [1] are said to be *thermally annealed*, which should lead to negligible redistribution for Si.

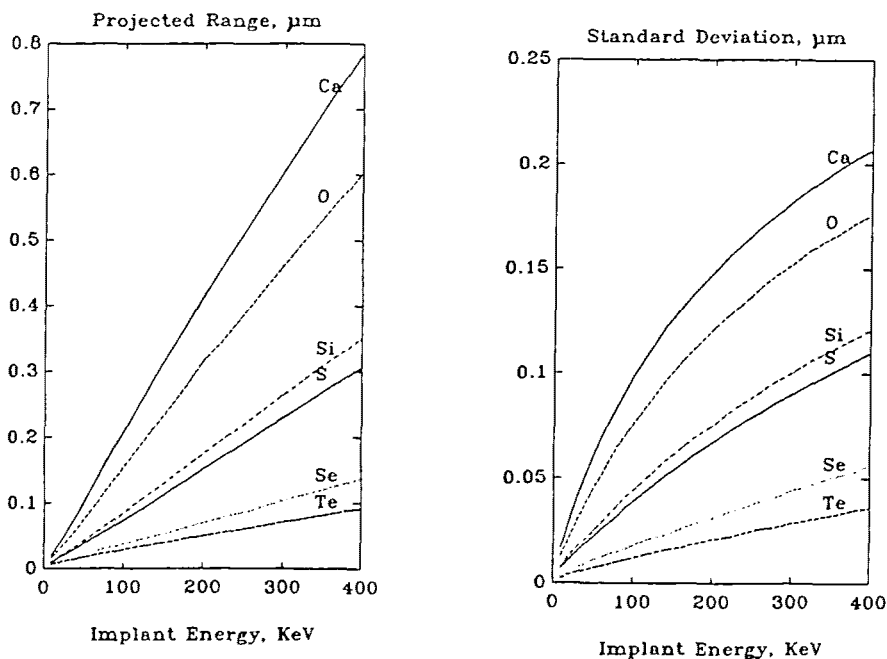


Figure 2: Projected range (left) and standard deviation (right) for implants on GaAs

faute de mieux in [13] (eq. 3.1-49) to estimate β should therefore be avoided, since it leads to $\beta < 3$ for small γ , and also fails for large γ to give acceptable values of β . An obvious modification could be:

$$\beta \approx 3 + 2.4\gamma^2 \quad (1)$$

which holds on the range $0 \leq \gamma \leq 5$. However, this expression leads, at least for Si implants, to smaller values than the optimum ones. In all computations both β and γ were assumed as a constant average value ($\gamma \approx 0.12$, $\beta \approx 12.5$). The Pearson IV fit of the profiles presented in [1] is shown in Fig.4.

Profile reshaping due to diffusion during annealing can be approximately dealt with by rescaling σ_p . Nevertheless, since Si implants thermally annealed show a practically negligible amount of diffusion ([1,8]), this phenomenon has not been considered in the simulations shown here. Last but by no means least, the knowledge of *activation* η is fundamental in evaluating the final shape of the donor profile. Unfortunately, this parameter again is strongly process-dependent, and the underlying physics is both involved and not fully understood. As a general rule, activation is a *decreasing* function of implanted dose; moreover, the activated sheet carrier concentration tends to *saturate* for high doses [3,8]. For still higher doses, a *decrease* of the sheet carrier concentration has also been observed [5]. In order to account for activation when simulating the input doping profile, a simple empirical *activation curve* has been introduced, which gives the activated sheet carrier concentration N_{sheet} as a function of the implanted dose D . Such a

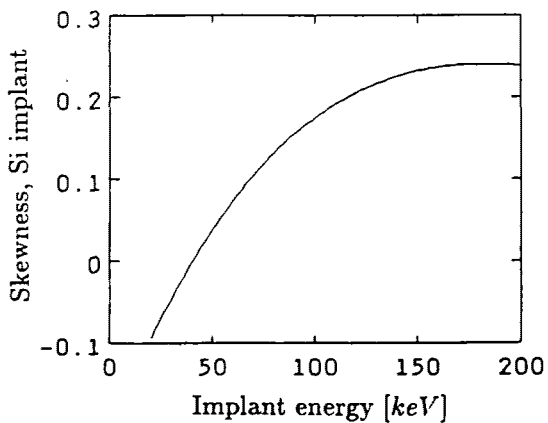


Figure 3: Skewness of Si on GaAs

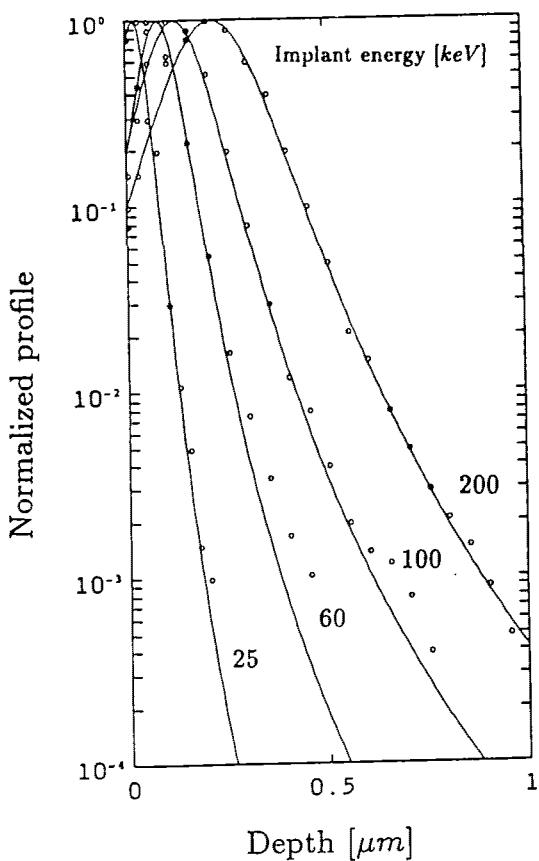


Figure 4: Pearson IV fits of Si implants on GaAs

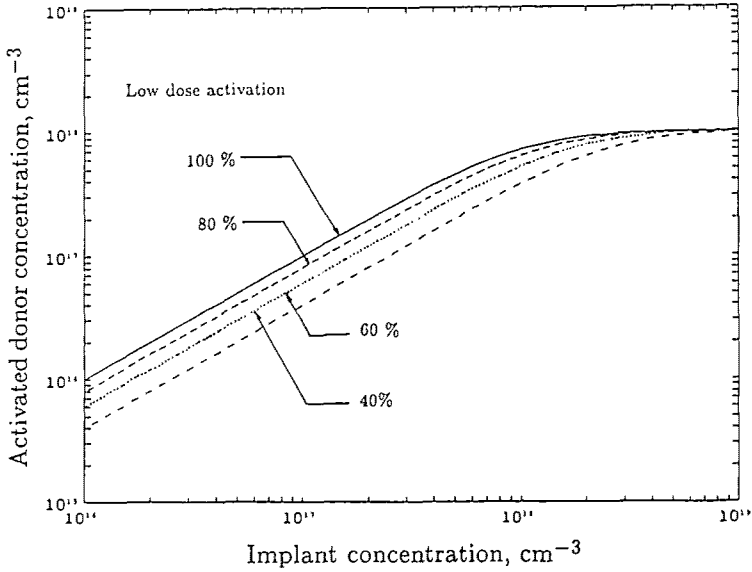


Figure 5: Activation curve

function is characterized by two parameters: the *low-dose activation* η_0 and the *saturation dose* D_{sat} , and has been approximated as:

$$N_{sheet} = \frac{\eta_0 D}{\sqrt{1 + (\eta_0 D / D_{sat})^2}} \quad (2)$$

Notice, however, that if activation is a *microscopic* process rather than an overall one, the relationship (2) should involve the dopant distribution $N_D(y)$ for *each* y rather than the overall sheet concentration only. To this aim, a similar curve has been introduced:

$$N_D(y) = \frac{\eta_0 N_{Di}(y)}{\sqrt{1 + (\eta_0 N_{Di}(y) / N_{Dsat})^2}} \quad (3)$$

where N_{Di} is the donor concentration with full activation, N_{Dsat} the solid solubility of the dopant in GaAs. A plot of Eq. 3 is shown in Fig. 5 for several values of the low-dose activation η_0 .

Low dose activations of 60-80 % and solid solubility limits of the order of 10^{18} cm^{-3} lead to fairly good agreement with measured profiles, as shown in Fig.6 for a double Si implant. The implant characteristics are: for the shallow implant, $D_1 = 1 \times 10^{13} \text{ cm}^{-2}$, $E_1 = 40 \text{ KeV}$; for the deep implant, $D_2 = 5 \times 10^{12} \text{ cm}^{-2}$, $E_2 = 120 \text{ KeV}$. Dots are measured data (SELENIA).

3 Effect of background impurities

Both epitaxial and ion-implanted devices are affected by the presence of residual background impurities. In state-of-the-art *epitaxial* MESFETs the intrinsic

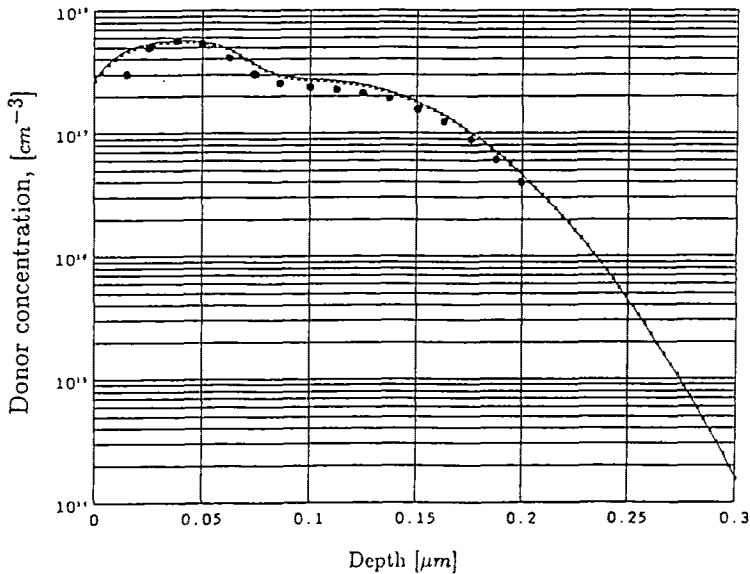


Figure 6: Measured and simulated double-implant profile

substrate shows a very low level of residual donors (mainly EL2) and acceptors (mainly carbon), of the order of 10^{14} cm^{-3} . A more significant role is played by *traps* present at the interface between the active layer and the substrate. In *implanted* devices, however, the non-abrupt doping profile and the increased amount of crystal damage arising from implantation makes background impurities significant, above all near pinch-off. Impurity levels N_T of the order of 10^{16} cm^{-3} are quite common; it is clear that in the tail of the doping distribution the concentration of ionized traps can be comparable or even greater than the one of the implanted donors. The situation is even worse when substrates intentionally doped with Chromium (an acceptor) so as to improve their semi-insulating properties are used; in this case, Cr levels of $2 \times 10^{16} \text{ cm}^{-3}$ can be found. This technology, however, is now less popular than it used to be a few years ago.

Let us confine ourselves in the following discussion to the case, wherein the substrate is still of *n-type*. This is almost certainly the case when *intrinsic* (i.e. not Cr-doped) substrates are used. The presence of a pn junction between the active layer and the substrate obviously requires the introduction of a two-carrier model including the hole continuity equation, unless the acceptor level in the p region is so low to render this region almost intrinsic.

If the hypothesis of *n-type* structure, a simple treatment of the effect of background impurities on Poisson equation is obtained if such impurities are introduced, with their own statistics, in the right-hand side of this equation. However, the presence of background impurities plays also a role in affecting the *transport properties* of carriers. The overall effect is that the *initial mobility* and the *saturation velocity* of carriers are strongly reduced when the compensation ratio $\theta = N_T(y)/N_D(y)$ is close to unity [15,7,10]. The underlying physics is examined

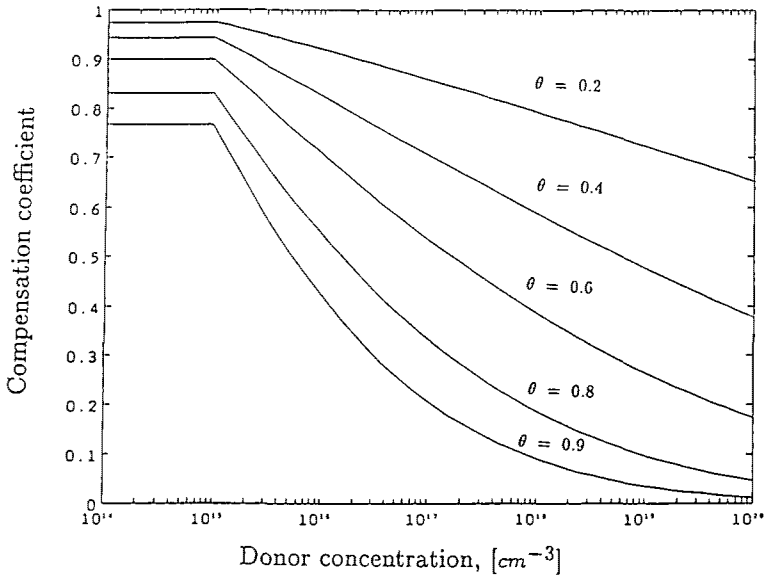


Figure 7: Effect of background impurities on mobility and saturation velocity

e.g. in [15]; here we only remark that the initial mobility profile turns out to be a non-monotonic function which *decreases* in the substrate, rather than *increasing* in correspondence of lower doping [4].

A simple model for the transport properties in the presence of background impurities (either donors or acceptors), which has been implemented in the MESS simulator, has been derived in [7] from the theory and data of [15]. According to this model, the initial mobility is approximated as:

$$\mu_0(y) = \frac{0.835}{1 + [\log(N_D(y))/23.25]^{23}} (1 - \theta)^b \quad (4)$$

where all quantities are in MKS units and the logarithm is *decimal*. The parameter b reads:

$$b = \begin{cases} 0.025(\log(N_D))^2 - 0.817 \log(N_D) + 6.25 & N_D > 10^{21} \text{ m}^{-3} \\ 0.115 & N_D < 10^{21} \text{ m}^{-3} \end{cases} \quad (5)$$

Similarly, for the saturation velocity the factor $\Psi = (1 - \theta)^b$ is supposed to be applied to the value which v_{sat} assumes in the absence of background impurities. A plot of this factor is shown in Fig. 7.

It ought to be noted that if the compensation ratio θ is unity, both carrier mobility and saturation velocity go to zero. This unphysical condition is avoided whenever, as already mentioned, the substrate does never become of p-type. With this limitation, the model of eq. 4 leads to a better agreement with measured DC curves near pinch-off than the simple Hilsum model [4]. For the sake of brevity, results on this point are omitted and will be presented elsewhere.

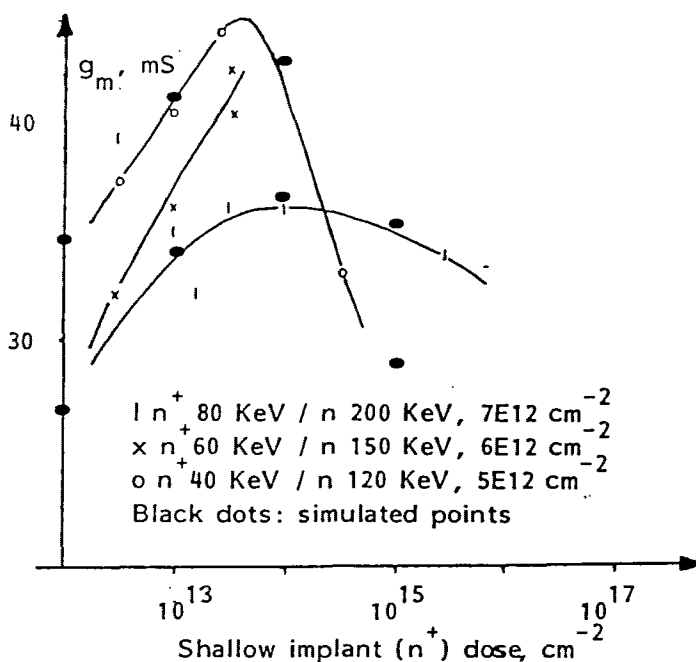


Figure 8: Double-implant MESFET transconductance

4 Profile optimization

Profile optimization has been performed on a class of double-implant recess-gate $0.5\mu\text{m} \times 300\mu\text{m}$ devices by varying the dose of the shallow implant. Double-implant MESFETs have been experimentally shown to achieve greater low-bias transconductance than simple implant devices. In fact, the curve g_m vs. the shallow implant dose shows a maximum (see Fig.8) whose location depends in turn on the energy and dose of the deep implant. The recess has been etched so as to maintain the saturation current of the device approximately constant.

In order to understand the reason of such a maximum, one should take into account that the device transconductance g_m can be expressed as:

$$g_m = \frac{g_{m0}}{1 + R_S g_{m0}} \quad (6)$$

where g_{m0} is the transconductance of the *intrinsic* device, R_S the source parasitic resistance. A double implant including a shallow n^+ implant reduces R_S and therefore increases g_m . Note that the gate recess is roughly positioned on the transition between the shallow and the deep implant when the two implants have widely different energies. However, when the dose of the shallow implant goes beyond a certain value, no significant further improvement on R_S is felt. On the other hand, the two implants begin to merge, and the gate must be more deeply recessed in order to obtain a constant saturation current. However, in this way the gate is positioned in a region where the profile is sharply decreasing, thereby leading to a poorer control of the current and to lower g_{m0} . If the gate

recess is kept constant, higher and higher transconductances are obtained, since the current levels are steadily increasing. Double-implant devices have better performances on g_m than single-implant ones, since the values of R_S and g_{m0} can be independently controlled, at least up to a certain extent.

To perform profile optimization, a set of profiles (Fig. 9) has been simulated. Since the physical simulator is comparatively CPU intensive, a preliminary coarse optimization has been performed through a quasi-two-dimensional simulator where the Poisson-Boltzmann equation is solved in one dimension. However, an accurate evaluation of R_S , which turns out to be a very sensitive parameter in planar devices, can only be achieved through a two-dimensional model where the non-unidimensional current flow is exactly described. It is also important to include in the model a surface depletion layer due to the presence of surface states [6]. The results obtained (Fig. 8) are in good agreement with measurements. Two-dimensional simulations were not performed on the second curve, since no experimental data were available beyond the maximum. Further investigations are required in order to be able to perform an overall profile optimization of the device also including as a goal other small-signal parameters relevant to the frequency behaviour (such as C_{GS}).

5 Conclusions

A few issues concerning the physical simulation of ion-implanted MESFET devices have been addressed. It has been shown that good fits of the input doping profiles can be obtained through Pearson IV distributions, and empirical solutions have been suggested for the simulation of activation. Simple models for the transport properties in the presence of residual impurities have been suggested, and an example of profile optimization has been given. Further work will concern the extension of the optimization to other small-signal parameters, and to the device bandwidth.

References

- [1] R. Anholt, T.W. Sigmon, M.D. Deal, "Process and devices models for GaAs MESFET technology", Technical Digest of 1987 GaAs IC Symp., pp.53-56, Portland, Oct.1987.
- [2] J.L. Cazaux, J. Graffeuil, "Optimisation du profil de dopage d'un MESFET réalisé par implantation ionique", *Revue Phys. Appl.*, vol.21, p.139, 1986.
- [3] A. Cetronio, M. Bujatti, P.D'Eustacchio, S. Ciceroni, "Rapid isothermal annealing of Si implanted semi-insulating GaAs by means of high frequency induction heating", in *Proc. Laser-Solid Interactions and Transient Thermal Processing of Materials*, Boston, MA, USA 1-4 Nov. 1982, p.641, Elsevier, New York.
- [4] C. Hilsum, "Simple empirical relationship between mobility and carrier concentration", *Electronics Letters*, vol.10, No.13, p.259, 27th June 1974.

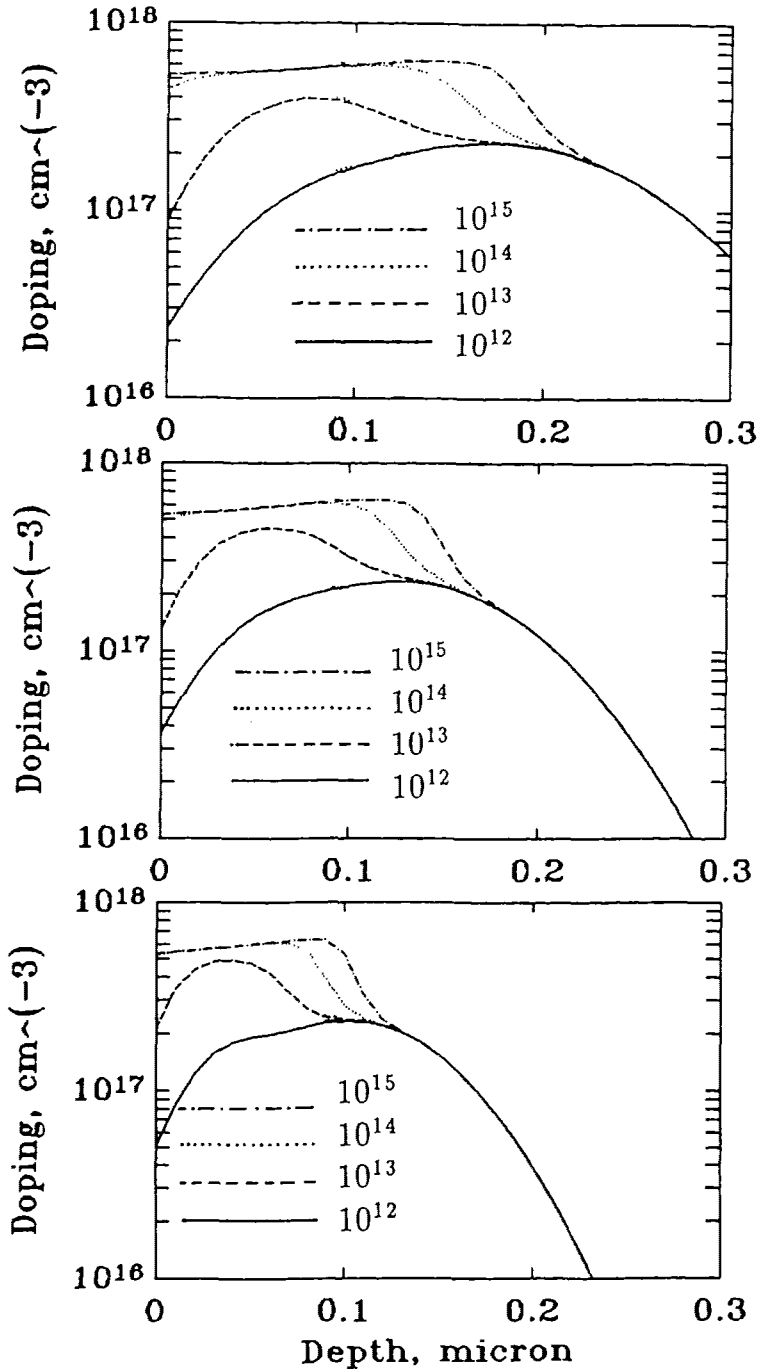


Figure 9: Simulated double-implant profiles

- [5] D.B.Gasson, I.C.Jennings, J.E.Parrot, A.N.Penn, in Proc. 6th Int. Conf. Semicond., p.681, Exeter 1962, Inst. of Phys. and Phys. Soc. London 1962.
- [6] G.Ghione, C.U.Naldi, F.Filicori, M.Cipelletti, G.Locatelli, "MESS - A two dimensional physical device simulator and its application to the development of C-band power GaAs MESFETs", *Alta Frequenza*, Special Issue on Microwave CAD, May 1988.
- [7] J.M.M.Golio, R.,J.Trew, "Profile studies of ion-implanted MESFET's", *IEEE Trans. on Electron Devices*, vol. ED-30, No.12, p.1844, Dec. 1983.
- [8] S.G.Liu, E.C.Douglas, C.P.Wu, C.W.Magee, S.Y.Narayan, S.T.Jolly, F.Kolondra, S.Jain, "Ion implantation of sulfur and silicon in GaAs", *RCA Review*, vol.41, p.227, June 1980.
- [9] D.Pavlidis, J.L.Cazaux, J.Graffeuil, "The influence of ion-implanted profiles on the performance of GaAs MESFET's and MMIC amplifiers", *IEEE Trans. on Microwave Theory and Techniques*, vol. ED-36, No.4, p.642, April 1988.
- [10] M.Pillan, F.Vidimari, A.M.Orsucci, "Dependence of mobility profiles on doping transition and impurity concentration in GaAs FET structures", *Proc. 4th Conf. on Semi-insulating III-V Materials - Hakone (Japan)*, May 1986.
- [11] H.Ryssel, "Implantation and diffusion models for process simulation", in *Proceedings VLSI Process and Device Modelling*, p 1, Catholic University of Leuven, 1983.
- [12] H.Ryssel, K.Haberger, K.Hoffmann, G.Prinke, R.Dumcke, A.Sachs, "Simulation of doping processes", *IEEE Trans. on Electron Devices*, Vol. ED-27, No.8, pp.1484, August 1984.
- [13] S.Selberherr, *Analysis and Simulation of Semiconductor Devices*, Springer Verlag, Wien 1984.
- [14] R.J.Trew, M.A.Khatibzadeh, N.A.Masnari, "Deep level and profile effects upon low-noise ion-implanted GaAs MESFET's", *IEEE Trans. on Electron Devices*, vol. ED-32, No.5, p.877, May 1985.
- [15] W.Walukiewicz, L.Lagoaski, L.Jastrzebski, M.Lichtensteiger, H.C.Gatos, "Electron mobility and free-carrier absorption in GaAs: Determination of the compensation ratio", *J. Appl. Phys.*, Vol.50, p.899, Feb.1979.
- [16] R.E.Williams, *Gallium arsenide processing techniques*, Artech House, Dedham (MA), 1984.